NASA CONTRACTOR REPORT

NASA CR-1800

IMPERFECTION SENSITIVITY OF OPTIMUM STRUCTURAL DESIGNS FOR A MARS ENTRY CAPSULE

by Gerald A. Cohen

Prepared by
PHILCO-FORD CORPORATION
Newport Beach, Calif. 92663
for Langley Research Center

NATIONAL AERONAUTICS AND SPACE ADMINISTRATION • WASHINGTON, D. C. • JUNE 1971

1. Report No. NASA CR-1800	2. Government Accession No.	3. Recipient's Catalog No.
4. Title and Subtitle **Imperfection Sensitivity of Optimum Structural Designs for a Mars Entry Capsule**		5. Report Date June 1971 6. Performing Organization Code
7. Author(s) **Gerald A. Cohen**		8. Performing Organization Report No. **None**
9. Performing Organization Name and Address **Philco-Ford Corporation** **Space and Reentry Systems Division** **Newport Beach, California 92663**		10. Work Unit No. 11. Contract or Grant No. NAS1-5554-8
12. Sponsoring Agency Name and Address National Aeronautics and Space Administration Washington, D.C. 20546		13. Type of Report and Period Covered **Contractor Report** 14. Sponsoring Agency Code
15. Supplementary Notes		

16. Abstract

The imperfection sensitivity of the buckling modes of eight shell configurations, six of which correspond to optimized capsule configurations for Mars entry, has been analytically evaluated. The theory used is a generalization of the Koiter imperfection theory to include nonlinear pre-buckling states, live loading, and arbitrary imperfection shapes. Results are presented in the form of charts of snapping load as a function of root-mean-square angular imperfection amplitude.

17. Key Words (Suggested by Author(s))	18. Distribution Statement
Imperfection Sensitivity **Buckling of conical shells** **Mars Entry capsules**	**Unclassified - Unlimited**

19. Security Classif. (of this report)	20. Security Classif. (of this page)	21. No. of Pages	22. Price*
Unclassified	**Unclassified**	31	$3.00

*For sale by the National Technical Information Service, Springfield, Virginia 22151

PREFACE

This study was initiated while the author was employed by the Philco-Ford Corporation. Technical responsibility for the completion of the work and the preparation of this report resides in Structures Research Associates under subcontract to Philco-Ford.

CONTENTS

SUMMARY	1
INTRODUCTION	2
SYMBOLS	3
RESULTS	4
120° Sandwich Cone (Ref. 15)	5
120° Ring-Stiffened Cone (Ref. 15)	6
120° Sandwich Cone (Ref. 16)	7
120° Ring-Stiffened Cone (Ref. 16)	7
0A.833 Tension Shell (Ref. 16)	8
140° Sandwich Cone (Ref. 17)	8
60° Sandwich Spherical Dish (Ref. 17).	9
0A.65 Tension Shell (Ref. 17).	9
Entry Capsule Configuration Comparison	9
CONCLUDING REMARKS	10
REFERENCES	11
TABLES	13
FIGURES	19

IMPERFECTION SENSITIVITY OF OPTIMUM STRUCTURAL DESIGNS FOR A MARS ENTRY CAPSULE

by

Gerald A. Cohen

Structures Research Associates, Newport Beach, California

SUMMARY

The imperfection sensitivity of the buckling modes of six optimized Mars entry capsule configurations has been analytically evaluated. The capsule configurations treated (120° and 140° blunted cones and a 60° spherical dish of sandwich construction, and 120° blunted cone and 0A.833 and 0A.65 tension shells of ring-stiffened construction) were obtained in previous studies. In addition, the buckling modes of two nonoptimum 120° truncated cones, one of sandwich and the other of ring-stiffened construction, also previously studied, have been evaluated. The analysis is based on nonlinear Novozhilov-type shell and ring theory and was performed with the aid of an initial postbuckling digital computer program developed for general ring-stiffened shells of revolution. In each case the calculations were based on nonlinear prebuckling equilibrium states, and additionally in the case of the two 120° truncated cones, on live normal pressure loading.

Results are presented in the form of charts of snapping load versus root-mean-square amplitude of angular shell and ring imperfections for two hypothetical imperfection shapes, one being proportional to the buckling mode deflections and the other producing the greatest possible loss of stability for sufficiently small imperfection amplitudes. The range of imperfection amplitudes presented is 0 to 5 milliradians, as the theory is valid only for small imperfections. The knockdown factors resulting from an assumed nominal imperfection amplitude of 5 milliradians are:

0.88 (120° sandwich cone), 0.82 (140° sandwich cone)
0.72 (60° spherical dish), 0.66 (0A.65 tension shell)
0.62 (120° ring-stiffened cone), and 0.57 (0A8.33 tension shell)

INTRODUCTION

In Reference 1 the theory is developed and a computer program is presented for the evaluation of the imperfection sensitivity of unique bifurcation buckling modes of ring-stiffened shells of revolution. The method presented there is an application of the imperfection analysis presented in References 2 and 3, which translates the original Koiter theory (Refs. 4-6), into the notation of Budiansky and Hutchinson (Refs. 7 and 8) and includes nonlinear prebuckling states, live loading, and arbitrary imperfection shapes. There exist in the literature several previous applications of Koiter's theory to specific shells (e.g., Refs. 9-11), and in References 12-14 nonlinear prebuckling states were included in the buckling and postbuckling analyses. Generally, in previous studies, the end product of the analysis has been the second postbuckling coefficient b (or the initial postbuckling stiffness) of the perfect shell, which, for buckling modes normalized to have a normal deflection amplitude equal to the shell thickness, is taken as a measure of the degree of imperfection sensitivity.

The present study makes use of the method presented in Reference 1 to evaluate eight shell configurations previously studied in References 15, 16, and 17. All of these shells have ring stiffeners, which are treated discretely. In the only previous treatment of ring-stiffeners (Ref. 9), the ring stiffness was uniformly distributed over the shell. In addition to computing the second postbuckling coefficient for each buckling mode, the first and second imperfection parameters, α and β, are computed for two imperfection shapes - one proportional to the buckling mode deflections, and the other producing the maximum value of α (and consequently the greatest loss of buckling strength) for any given value of the root-mean-square amplitude of angular shell and ring imperfections. From these results charts are made of the snapping load versus imperfection amplitude.

In this study possible interactions between two or more buckling modes of the perfect structure are neglected. Also, as noted in Ref. 2 other terms of the order of the β-terms have been tacitly neglected in the development of the first-order imperfection theory. However, the extent to which nonzero β-values affect the predicted knockdown factors is indicative of the error in the first-order theory.

SYMBOLS

b	second postbuckling coefficient
N	circumferential harmonic number
p	pressure
W_R	residual weight available for landed payload
W_S	total structure plus heatshield weight
α	first imperfection parameter
β	second imperfection parameter
η	buckling load knockdown factor
λ	load factor
$\bar{\xi}$	root-mean-square amplitude of angular shell and ring imperfections

Subscripts:

c	critical value for perfect structure
s	critical value for imperfect structure
mode	pertaining to the imperfection shape proportional to the mode displacements

Superscripts:

$\wedge$	pertaining to the imperfection shape which maximizes α
$*$	evaluated at the bifurcation point

RESULTS

The eight shell configurations treated are defined in detail in References 15, 16 and 17 and any changes in the details presented there are noted below. For the designs of Reference 16, only the low temperature (300°F), low ballistic coefficient (0.32 slug/ft^2) capsule designs are considered. The method of analysis is presented in Reference 1, and only final results are presented here.

The snapping load λ_s is defined as the relative maximum attained by the load factor λ (proportional loading is assumed) with respect to deflection for equilibrium states of an imperfect structure. In the case of axisymmetric structures which buckle in a unique harmonic mode, this relative maximum exists for small imperfections if the postbuckling coefficient b is negative. Also, in this case the perfect structure exhibits a postbuckling load drop-off after bifurcation. The parameters α and β depend on the specific imperfection displacement distribution assumed, and in cases of negative b determine along with the value of b the severity of the buckling load knockdown. In this study, two imperfection shapes were considered - one proportional to the perfect structure buckling mode, and the other yielding, for a given value of the mean square angular imperfection amplitude $\bar{\xi}^2$, the maximum possible value of α, and consequently for sufficiently small imperfections, the smallest value of λ_s.

The basic equation relating the ratio of snapping load λ_s of an imperfect structure to bifurcation load λ_c of the corresponding perfect structure with the root-mean-square angular imperfection amplitude $\bar{\xi}$ for various values of the parameters b, α, and β is given as Eq. (3) of Reference 1 and displayed there as Figure 1. Because of its fundamental importance this relation is reproduced here also as Figure 1. Two observations pertinent to Figure 1 are noted. First, for $\beta/\alpha \geq 1$, λ_s/λ_c approaches from above the horizontal asymptote $(\beta/\alpha - 1)/(\beta/\alpha)$ for large values of $\bar{\xi}$, whereas for $\beta/\alpha < 1$, λ_s/λ_c becomes negative for large $\bar{\xi}$. This behavior of the curves of Figure 1 for large $\bar{\xi}$ clearly does not represent the real situation, and indeed this is consistent with the fact that the theory upon which this relationship is based is a first-order theory in $\bar{\xi}$. Thus the curves shown in Figure 1 are, in reality, asymptotes of the true curves for $\bar{\xi} \to 0$. Secondly, if based on linear prebuckling theory neglecting prebuckling rotations, the ratio β/α would equal unity.

In some cases, the independent treatment of certain higher buckling modes, i.e., in a harmonic $N \neq N_c$, is inaccurate because of the closeness of the eigenvalue in the harmonic N with that of the harmonic 2N. When this occurs, the differential equations for the 2N harmonic component of the second-order contribution to the postbuckled state are practically singular, and their solution is so large as to violate the order of magnitude assumptions

in the analysis. This is particularly evident in the results presented for the ring-stiffened shells for which inordinately large negative b-values were calculated as a result of this approximate singularity. In the case of the OA.833 tension shell a result attributable to this limitation of the independent mode analysis is so unrealistic that it is discarded (see p. 8) and not included in its load knockdown chart. In the cases of the ring-stiffened cones and the OA.65 tension shell, the largest negative b-values presented may also lead to inaccurate results, however, these results are included in the knockdown charts presented.

120° Sandwich Cone (Ref. 15)

The base and nose rings used in the present analysis of the sandwich and ring-stiffened cones of Reference 15 are not included in those discussed in that reference. They are instead tubular rings with 6.00 in. O.D. by 0.156 in. thick for the base ring and 2.50 in. O.D. by 0.125 in. thick for the nose ring. These edge rings were used for both the 120° sandwich and ring-stiffened cones.

In Table I are shown the essential results for the 120° sandwich cone of Reference 15. These results are based on live uniform pressure and a nonlinear prebuckling state at p = 6.20 psi.* Values of b, α, and β presented in Table I and the following tables are based on buckling modes normalized to have a normal deflection amplitude of one inch.** Note that for some harmonics, the lowest two modes were obtained. However, the complete analysis was carried through only for those modes which could conceivably control buckling of the imperfect structure.

Using these results and the knockdown relation illustrated in Figure 1, the critical pressure chart (Fig. 2) was constructed. As shown, the lowest buckling mode of the perfect structure (N = 7) controls the buckling of the imperfect structure for imperfection amplitudes less than roughly 0.0018 rad.

---

* It is noted that in the method used to compute the bifurcation buckling modes (Ref. 18) it is not necessary that the load λ_o at which the nonlinear prebuckling state is computed coincide with the bifurcation load λ_c. Good accuracy is obtained if λ_o is sufficiently close to λ_c so that the prebuckling state at bifurcation is approximated by the superposition of the nonlinear prebuckling state at λ_o and a linear perturbation state about it. In the postbuckling analysis all necessary prebuckling state variables (and their derivatives with respect to λ) are corrected, to first order in the difference $\lambda_c - \lambda_o$, to the bifurcation load λ_c.

** Note that the quantities $\alpha^2 b$ and β/α, which determine the snapping load (Fig. 1), do not depend on the normalization of the buckling mode.

For larger imperfection amplitudes, it is likely that the N = 6 mode would control.* For sufficiently small values of $\bar{\xi}$ the curve labeled max α imperfection gives the smallest possible critical load. The spread between the buckling mode imperfection and the maximum α imperfection curves is indicative of the effect of different imperfection shapes. The scale shown at the top of Figure 2 and succeeding figures relates the root-mean-square angular amplitude to the normal deflection amplitude for buckling mode imperfections. Thus, for example from Figure 2, an imperfection proportional to the N = 7 buckling mode with an RMS angular amplitude of one milliradian has a maximum normal reflection of 0.0175 inch.

120° Ring-Stiffened Cone (Ref. 15)

In Table II are shown the essential results for the 120° ring-stiffened cone of Reference 15. From the results shown it is seen that the effect of live pressure is more significant for the postbuckling coefficient b than it is for the critical pressure p_c. However, as it does for p_c, this effect on b diminishes with increasing harmonic number. Based on the live pressure results for N = 5 and 6 and the dead pressure results for N = 7, the critical pressure chart for the imperfect structure (Fig. 3) was constructed.** For the sake of clarity, the curve for the N = 7 buckling mode imperfection is omitted. It lies wholly above the corresponding maximum α imperfection curve in much the same manner as for N = 6 curves. In this case, for imperfections of moderate size the much smaller value of β for the N = 5 buckling mode imperfection overcomes the larger value of α for the maximum α imperfection, so that the buckling mode imperfection results in smaller critical pressures.

It is noted, however, that the computed values of β for this cone (and the ring-stiffened conical capsule discussed below) may not be as accurate as the β-values computed for the other structures. For the ring-stiffened cones the terms in the β-formula [Eq. (34b) of Ref. 3] which depend quadratically on prebuckling rotations appear to be dominant terms. Because of the current program limitation of 100 output points for shell response variables, the prebuckling rotation, which has a rapid

---

* Insofar as these and the following results, which neglect interactions between two or more buckling modes, indicate a nonfundamental mode controlling the buckling of the imperfect structure, significant mode interactions are possible.

** Strictly speaking, live uniform pressure is not conservative for a shell with edge rings, and is therefore beyond the scope of the initial post-buckling theory used (Ref. 2). However, it is probable that relative to a laboratory test of this shell, the live pressure results are more accurate than the corresponding dead pressure results.

variation between rings for the ring-stiffened cones, may not have been obtained with sufficient accuracy for these terms to be very accurate.* This loss of significance, if indeed it occurred, may be accentuated for the buckling mode imperfection, since for this imperfection the terms in question tend to cancel each other out. In order to check the accuracy of the β-values obtained for the ring-stiffened cones, the analysis for these shells should be repeated with more output points, with at least two or three output points between each adjacent ring pair.

As seen from Figure 3, for imperfection amplitudes less than roughly 0.0012 rad the N = 7 harmonic controls the buckling, although the closeness of the curves indicates that any one of the N = 5, 6, or 7 modes could be critical depending on the actual imperfection shape. For larger imperfections, the N = 5 mode appears to be critical.

120° Sandwich Cone (Ref. 16)

In Table III are shown the essential results for the 120° sandwich conical capsule (0.32 slug/ft^2, 300°F) presented in Reference 16. In this and the following cases the pressure distribution is nonuniform (treated as dead loading) and the applied load is characterized by the load factor λ which multiplies the expected peak dynamic pressure entry load. Thus λ is the safety factor for buckling failure, and $\lambda > 1$ corresponds to buckling loads greater than that expected during Mars entry. The results shown in Table III are based on a nonlinear prebuckling state at $\lambda = 2.48$. The corresponding snapping loads for imperfect shells are shown in Figure 4. As shown, only two imperfection-sensitive modes, N = 5 and 4 appear to play a role. It should be noted that in this and the following cases, the N = 2 mode could be eliminated from consideration simply by increasing the base ring stiffness.

120° Ring-Stiffened Cone (Ref. 16)

In Table IV are shown the essential results for the 120° ring-stiffened conical capsule (0.32 slug/ft^2, 300°F) presented in Reference 16. These results are based on a nonlinear prebuckling state at $\lambda = 2.16$. In Figure 5 are shown the corresponding snapping loads. These results are similar to the results for the ring-stiffened cone of Reference 15 (Fig. 3) in that for imperfection amplitudes of moderate size the buckling mode deflection appears to be the most detrimental imperfection shape.

* Only one output point between each adjacent ring pair was used.

0A.833 Tension Shell (Ref. 16)

In Table V are shown the essential results for the 0A.833 tension shell capsule (0.32 slug/ft^2, 300°F) presented in Reference 16. These results are based on a nonlinear prebuckling state at $\lambda = 2.25$. It should be noted that this design (and the 0A.65 tension shell design discussed below) has 90 stringers uniformly spaced around the shell circumference.* Since in the analysis the stringer stiffness is circumferentially smeared out, the results tend to lose significance for, say, $N > 20$. This is particularly true for the b-calculation, for which the harmonic 2N plays a role.

The extremely large negative b-value obtained for the N = 13 mode is spurious, resulting from the fact that the value of λ for N = 26 is very close to the value 2.48 for N = 13, as may be inferred from Table V. As a consequence the differential equations for the N = 26 harmonic component of the second-order contribution to the postbuckled state are practically singular, and their solution is so large as to violate the order of magnitude assumptions inherent in the analysis. A determination of the buckling load knockdown associated with the N = 13 mode therefore requires consideration of the interaction of this mode with the N = 26 mode, and such an analysis is beyond the scope of this study.

The snapping loads corresponding to the results of Table V are shown in Figure 6. The buckling mode imperfection curves are omitted for the sake of clarity. These lie wholly above the corresponding curves shown for the maximum α imperfections. For the reasons discussed above, no results are shown for the N = 13 mode. However, even without consideration of this mode, the results show a serious loss of stability due to imperfections. Consequently, this configuration probably should be redesigned in order to sustain the anticipated loads.

140° Sandwich Cone (Ref. 17)

In Table VI are shown the essential results for the 140° sandwich conical capsule presented in Reference 17. These results are based on a nonlinear prebuckling state at $\lambda = 2.00$. The corresponding snapping loads are shown in Figure 7. In this case, the critical buckling mode (N = 5) for the perfect structure has a stable postbuckling behavior. However, for imperfection amplitudes greater than roughly 0.001 rad, lower critical loads associated with the unstable N = 4 mode are possible.

---

* The stringers suppress the rapid variation of the prebuckling rotation between rings (cf. Figs. 17 and 21 of Ref. 16), thereby eliminating the possibility of a numerical loss of accuracy in the β-calculation noted earlier for the ring-stiffened cones.

60° Sandwich Spherical Dish (Ref. 17)

In Table VII are shown the essential results for the 60° sandwich spherical capsule presented in Reference 17. These results are based on a nonlinear prebuckling state at $\lambda = 2.10$. The corresponding snapping loads are shown in Figure 8. As shown, it is possible for either the N = 7, 6 or 5 modes to control the buckling depending on the size and shape of the imperfection.

OA.65 Tension Shell (Ref. 17)

In Table VIII are shown the essential results for the OA.65 tension shell capsule presented in Reference 17. These results are based on a nonlinear prebuckling state at $\lambda = 2.50$. The corresponding snapping loads are shown in Figure 9. As shown, for all but very small imperfections, the N = 11 mode would probably control. The N = 2 mode, which is just slightly sensitive to imperfections can be suppressed by increasing the base ring stiffness.

Entry Capsule Configuration Comparison

With the results presented in Figs. 2 - 9, Table III of Reference 17 can be enlarged to include the buckling safety factors for the six entry capsule configurations with geometric imperfections, as shown in Table IX. In this table, η is the knockdown factor by which the safety factor is reduced by the assumed imperfection. It is seen that the three sandwich capsules are less sensitive to geometric imperfections than are the three ring-stiffened capsules. This result is in apparent agreement with the results of previous studies (Refs. 6 and 13) which show that, in general, most methods for increasing the buckling load without an increase in structural weight tend to increase the imperfection-sensitivity as well.

If one insists on a 50% safety margin with the imperfection amplitude $\bar{\xi} = 0.005$ rad, all but two of these configurations would require redesign, the two suitable designs being the 120° and 140° sandwich cones. In order to make the comparison between these two configurations more meaningful, one can use Figure 28 of Reference 19 to adjust the structural weight of the 120° sandwich cone to a value compatible with the buckling load of the 140° sandwich cone. Assuming that the knockdown factor of 0.79 remains unchanged, one can compute a structural weight of approximately 561 lb for an optimum 120° sandwich cone which buckles at $\lambda_s = 1.58$ for $\bar{\xi} = 0.005$ rad. Although this is 7 lb less than the structural weight required for the 140° sandwich cone, the corresponding residual weight (W_R) is still only 3839 lb,

543 lb short of that attainable with the 140° sandwich cone. Thus, structurally, the 120° and 140° sandwich cones appear to be on a par, but the higher drag coefficient of the 140° cone makes this configuration the more favorable design. On the other hand, the structural weight of the 120° ring-stiffened cone adjusted to $\lambda_s = 1.58$ for $\bar{\xi} = 0.005$ rad is approximately 600 lb, resulting in a residual weight of 3800 lb, 39 lb less than that for the 120° sandwich cone. The effect of imperfections is therefore seen to lower the ballistic coefficient below which ring-stiffened construction is superior to sandwich construction.

CONCLUDING REMARKS

Critical load charts of eight geometrically imperfect shell configurations, six of which have previously been optimized for consideration as Mars entry capsules, have been presented. In general, the ring-stiffened designs are more sensitive to small geometric imperfections than are the sandwich designs. Of the candidate Mars capsule designs studied, only two, the 120° and 140° sandwich cones, retain at least a 50 percent margin of safety at a root-mean-square angular imperfection amplitude of 0.005 rad. Of these two, the 140° sandwich cone is favored because of its higher drag coefficient and, hence, residual weight available for landed payload.

The second imperfection parameter β apparently plays an important role in predicting the buckling loads of ring-stiffened shells at reasonable values of the imperfection amplitude. In some cases it can cause an imperfection shape proportional to the buckling mode displacements to be more detrimental than the imperfection shape with maximizes the first imperfection parameter α. However, the theory upon which β is based implicitly neglects other terms of the same order. Therefore, the asymptotic imperfection analysis should be systematically reconsidered to determine to what extent the snapping load expression including β should be altered.

A deficiency in the analysis upon which the foregoing results are based is the independent treatment of each of the buckling modes of the perfect structure. In those cases where nonfundamental modes appear to produce the critical load of the imperfect structure, it is likely that the interaction between two or more modes is not negligible. For such problems, which, from the results presented, appear to be common for practical structures, additional analysis is necessary.

REFERENCES

1. Cohen, G.A.: Computer Program for Analysis of Imperfection Sensitivity of Ring-Stiffened Shells of Revolution. NASA CR-1801, 1971.

2. Cohen, G. A.: Effect of a Nonlinear Prebuckling State on the Postbuckling Behavior and Imperfection Sensitivity of Elastic Structures. AIAA J., vol. 6, no. 8, August 1968, pp. 1616-1619.

3. Cohen, G. A.: Reply by Author to J. R. Fitch and J. W. Hutchinson. AIAA J. vol. 7, no. 7, July 1969, pp. 1407-1408.

4. Koiter, W. T.: On the Stability of Elastic Equilibrium (in Dutch with English summary). Thesis, Polytechnic Institute at Delft, H. J. Paris (Amsterdam), 1945; English translation, NASA TT F-10,833, 1967.

5. Koiter, W. T.: Elastic Stability and Post-Buckling Behavior. Nonlinear Problems. R. E. Langer, ed., University of Wisconsin Press, Madison, Wis., 1963.

6. Koiter, W. T.: General Equations for Elastic Stability for Thin Shells. Proceedings - Symposium on the Theory of Thin Shells. Univ. of Houston Press, 1967.

7. Budiansky, B.; and Hutchinson, J. W.: Dynamic Buckling of Imperfection Sensitive Structures. Proceedings of the XI International Congress of Applied Mechanics. H. Gortler, ed., Springer-Verlag, Berlin, 1964, pp. 636-651.

8. Budiansky, B: Dynamic Buckling of Elastic Structures: Criteria and Estimates. Dynamic Stability of Structures. G. Herrmann, ed., Pergamon Press, 1965, pp. 83-106.

9. Hutchinson, J. W.; and Amazigo, J. C.: Imperfection-Sensitivity of Eccentrically Stiffened Cylindrical Shells. AIAA J., vol. 5, no. 3, March 1967, pp. 392-401.

10. Hutchinson, J. W.: Initial Post-Buckling Behavior of Toroidal Shell Segments. Int. J. Solids Structures, vol. 3, 1967, pp. 97-115.

11. Danielson, D. A.: Buckling and Initial Postbuckling Behavior of Spheroidal Shells under Pressure. AIAA J., vol. 7, no. 5, May 1969, pp. 936-944.

12. Fitch, J. R.: The Buckling and Post-Buckling Behavior of Spherical Caps under Concentrated Load. Int. J. Solids Structures, vol. 4, 1968, pp. 421-446.

13. Hutchinson, J. W.; and Frauenthal, J. C.: Elastic Postbuckling Behavior of Stiffened and Barreled Cylindrical Shells. J. Appl. Mech., Paper No. 69-APM-U.

14. Fitch, J. R.: and Budiansky, B.: The Buckling and Post-Buckling Behavior of Spherical Caps under Axiymmetric Load. Presented at the 10th ASME/AIAA Structures, Structural Dynamics and Materials Conference, New Orleans, April 1969.

15. Cohen, G. A.: The Effect of Edge Constraint on the Buckling of Sandwich and Ring-Stiffened 120 Degree Conical Shells Subjected to External Pressure. NASA CR-795, May 1967.

16. Cohen, G. A.: Foster, R. M.; and Dowty, J. R.: Synthesis of Optimum Structural Designs for Conical and Tension Shell Mars Entry Capsules. NASA CR-1365, 1969.

17. Cohen, G. A.: Evaluation of Configuration Changes on Optimum Structural Designs for a Mars Entry Capsule, NASA CR-1414, 1969.

18. Cohen, G. A.: Computer Analysis of Asymmetric Buckling of Ring-Stiffened Orthoropic Shells of Revolution. AIAA J., vol. 6, no. 1, Jan. 1968, pp. 141-149.

19. Cohen, G. A.: Structural Optimization of Sandwich and Ring-Stiffened 120 Degree Conical Shells Subjected to External Pressure. NASA CR-1424, 1969.

TABLE I

120° SANDWICH CONE (Ref. 15)

N	P_c (psi)	b	$\hat{\alpha}$	$\hat{\beta}$	α_{mode}	β_{mode}
2	9.95	-5.50×10^{-5}	128.6		48.5	
3	~26					
4	13.75	0.030				
5	8.78	1.124				
6	6.99	-0.218	30.2	38.9	20.7	19.8
7	6.63	-0.079	25.6	30.3	18.8	18.3
	51.8					
8	6.90	0.011				
9	7.49	0.088				
	29.8					
11	9.20	0.231				
	26.25					

TABLE II

120^{o} RING STIFFENED CONE (REF. 15)

N	$p_c^{(a)}$ (psi)	$p_c^{(b)}$ (psi)	$p_c^{(c)}$ (psi)	$\frac{(a)}{b}$	$\frac{(b)}{b}$	$\frac{(c)}{b}$	$\frac{(a)}{\hat{\alpha}}$	$\frac{(b)}{\hat{\alpha}}$	$\frac{(c)}{\hat{\alpha}}$	$\frac{(a)}{\hat{\beta}}$	$\frac{(b)}{\hat{\beta}}$	α mode (a)	α mode (b)	α mode (c)	β mode (a)	β mode (b)
2			9.49			3.02×10^{-3}										
3			15.6			1.18										
4	8.69	8.63	8.84	-0.034	-0.019	-0.030	34.4	35.1	33.4			16.5	16.6	16.3		
5	5.21	5.18		-39.2	-16.8		24.0	24.2		53.9	53.6	15.0	15.1		12.4	12.4
6	4.23	4.22 14.03		-0.594	-0.586		19.2	19.3		31.6	31.6	13.9	13.9		13.2	13.2
7	4.11	4.11 10.36		-0.465			17.2			25.6		13.1			12.8	
8	4.30	4.30 9.34		-0.357			16.7					12.8				
9			9.59													
10	5.24			0.030												
12	6.72			0.424												

[a]Based on dead pressure and a nonlinear prebuckling state at p = 4.20 psi.

[b]Based on live pressure and a nonlinear prebuckling state at p = 4.00 psi.

[c]Based on live pressure and a nonlinear prebuckling state at p = 8.00 psi.

TABLE III

120^{o} SANDWICH CONE (Ref. 16)[a]

N	λ_c	b	$\hat{\alpha}$	$\hat{\beta}$	α_{mode}	β_{mode}
2	2.18	3.09×10^{-5}				
3	4.04					
4	2.82	-0.189	52.3	63.9	33.0	32.3
5	2.44	-0.0452	40.0	44.0	28.9	28.6
6	2.54	-0.0114	33.3	35.0	26.0	25.9
8	3.18					
10	4.11					

TABLE IV

120^{o} RING-STIFFENED CONE (Ref. 16)

N	λ_c	b	$\hat{\alpha}$	$\hat{\beta}$	α_{mode}	β_{mode}
2	2.19	-1.93×10^{-3}	212.6	581.	61.6	58.5
3	3.52	-0.17	65.8		19.7	
4	2.28	-3.17	41.0	258.	18.1	13.3
5	2.08	-0.32	29.8	179.	15.4	14.1
6	2.17	0.06				
7	2.22	0.45				
9	2.58	1.11				
11	3.47	2.04				

[a]The stability safety factors shown in this and the following tables show slight deviations from those reported in References 16 and 17 due primarily to the more precise heatshield weights (and hence inertial loads) used in the present prebuckling state calculations.

TABLE V

OA.833 TENSION SHELL (Ref. 16)

N	λ_c	b	$\hat{\alpha}$	$\hat{\beta}$	α_{mode}	β_{mode}
2	2.16	-2.22×10^{-3}	210.7	272.	46.6	43.6
3	4.77					
4	5.76					
6	5.51					
8	4.16					
10	3.14	1.4				
12	2.63	7.2				
13	2.48	-295.[a]	25.7	32.4	11.8	10.3
14	2.38	-6.74	23.6	28.7	11.5	10.2
15	2.32	-2.65	21.8	25.6	11.1	10.0
16	2.28	-0.969	20.3	23.1	10.9	9.94
17	2.262	0.0018				
18	2.263	0.656				
20	2.30	1.45				
24	2.44					

TABLE VI

140° SANDWICH CONE (Ref. 17)

N	λ_c	b	$\hat{\alpha}$	$\hat{\beta}$	α_{mode}	β_{mode}
2	2.06	-1.23×10^{-3}	163.1	259.	61.8	56.0
3	3.40					
4	2.27	-0.133	73.6	122.	37.9	35.7
5	1.93	0.026				
6	1.98	0.074				
8	2.46					
10	3.17					

[a] This value is spurious due to the closeness of λ_c for N=26 to 2.48 (cf discussion on Page 8).

TABLE VII

60^{o} SANDWICH SPHERICAL DISH (Ref. 17)

N	λ_c	b	$\hat{\alpha}$	$\hat{\beta}$	α_{mode}	β_{mode}
2	2.08	3.26×10^{-4}				
3	4.35					
4	3.13					
5	2.36	-0.576	45.0	64.4	34.0	29.3
6	2.09	-0.168	36.2	44.4	29.4	25.8
7	2.06	-0.121	31.0	35.1	26.2	23.8
8	2.15	-0.092	27.5	29.9	23.9	22.3
9	2.33					
11	2.84					

TABLE VIII

OA.65 TENSION SHELL (Ref. 17)

N	λ_c	b	$\hat{\alpha}$	$\hat{\beta}$	α_{mode}	β_{mode}
2	2.22	-1.23×10^{-4}	227.0	392.	48.5	41.4
3	3.34					
4	4.18					
6	4.07					
9	3.05					
10	2.84	6.81				
11	2.71 3.97	-5.08	24.5	29.6	13.2	12.5
12	2.62	-1.04	22.7	26.5	12.8	12.2
13	2.58	-0.115	21.1	24.0	12.4	11.9
14	2.561 3.79	0.38				
15	2.565	0.70				
17	2.61 3.94	1.05				
18	2.65					
21	2.77					

TABLE IX

BUCKLING SAFETY FACTORS FOR IMPERFECT CAPSULE CONFIGURATIONS FOR MARS ENTRY[a]

Configuration	W_S (lb)	W_R (lb)	$\bar{\xi}$ = 0.0025 rad		$\bar{\xi}$ = 0.005 rad		Adjusted Weights[c]	
			λ_s	η	λ_s	η	W_S	W_R
120° Sandwich cone[b]	585	3815	2.12	0.97 (0.87)	1.92	0.88 (0.79)	561	3839
140° Sandwich cone	568	4382	1.75	0.91	1.58	0.82		
60° Sandwich spherical dish	515	4065	1.72	0.83	1.48	0.72		
OA.65 Tension shell[b]	597	4828	1.76	0.79 (0.69)	1.46	0.66 (0.57)		
120° Ring-stiffened cone	559	3841	1.60	0.77	1.29	0.62	600	3800
OA.833 Tension shell[b]	605	4595	1.51	0.70 (0.67)	1.24	0.57 (0.55)		

[a]Based on orbit entry with a ballistic coefficient of 0.32 slug/ft^2.

[b]For these shells, the N=2 mode is critical for the perfect shell, and consequently the η-factors are based on the N=2 buckling loads at $\bar{\xi}$=0. The knockdown factors neglecting the N=2 modes are given in parentheses.

[c]Adjust to λ_s = 1.58 for $\bar{\xi}$ = 0.005 rad using results of Reference 19.

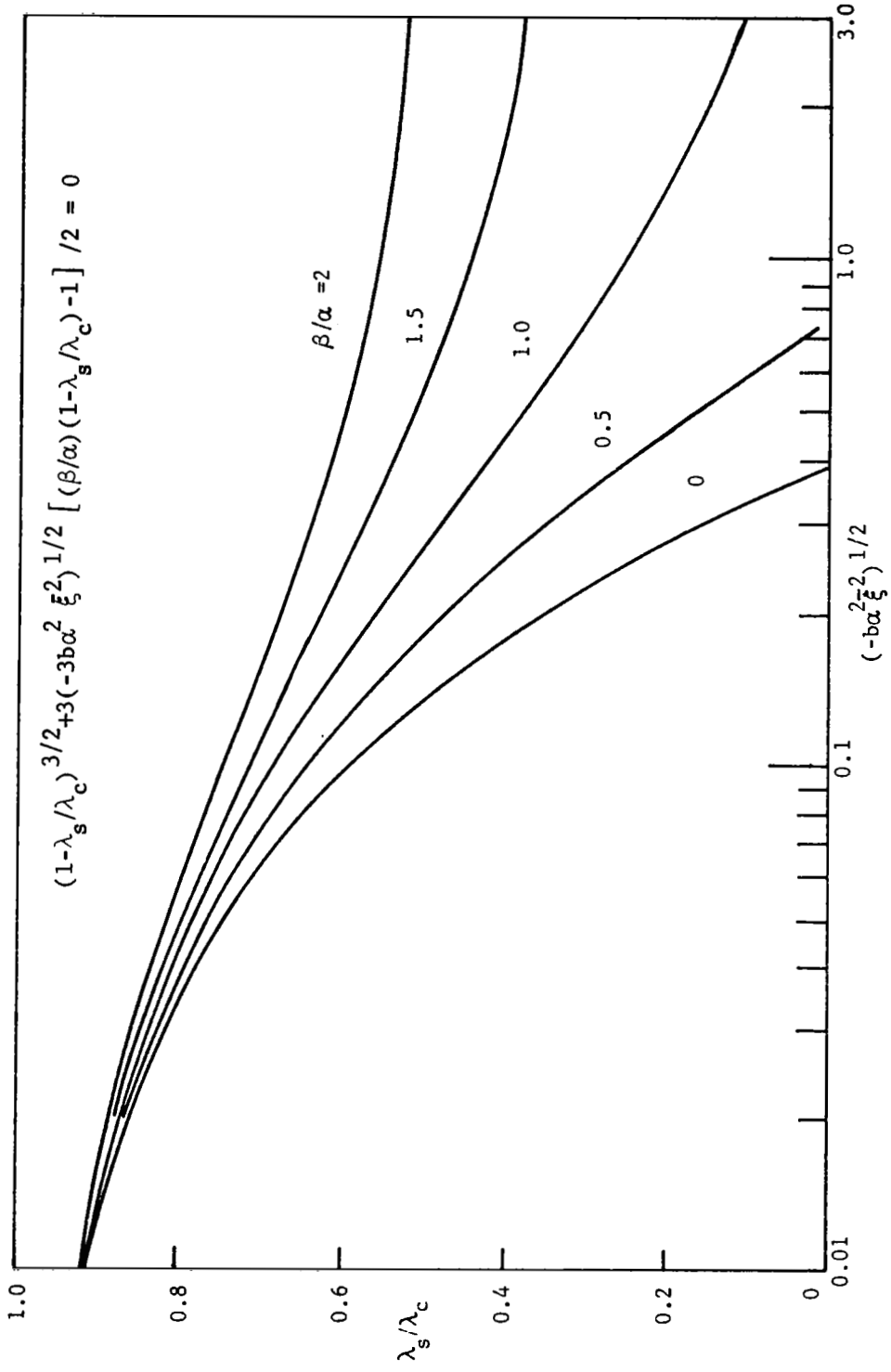

FIGURE 1. CRITICAL LOADS OF IMPERFECTION SENSITIVE STRUCTURES

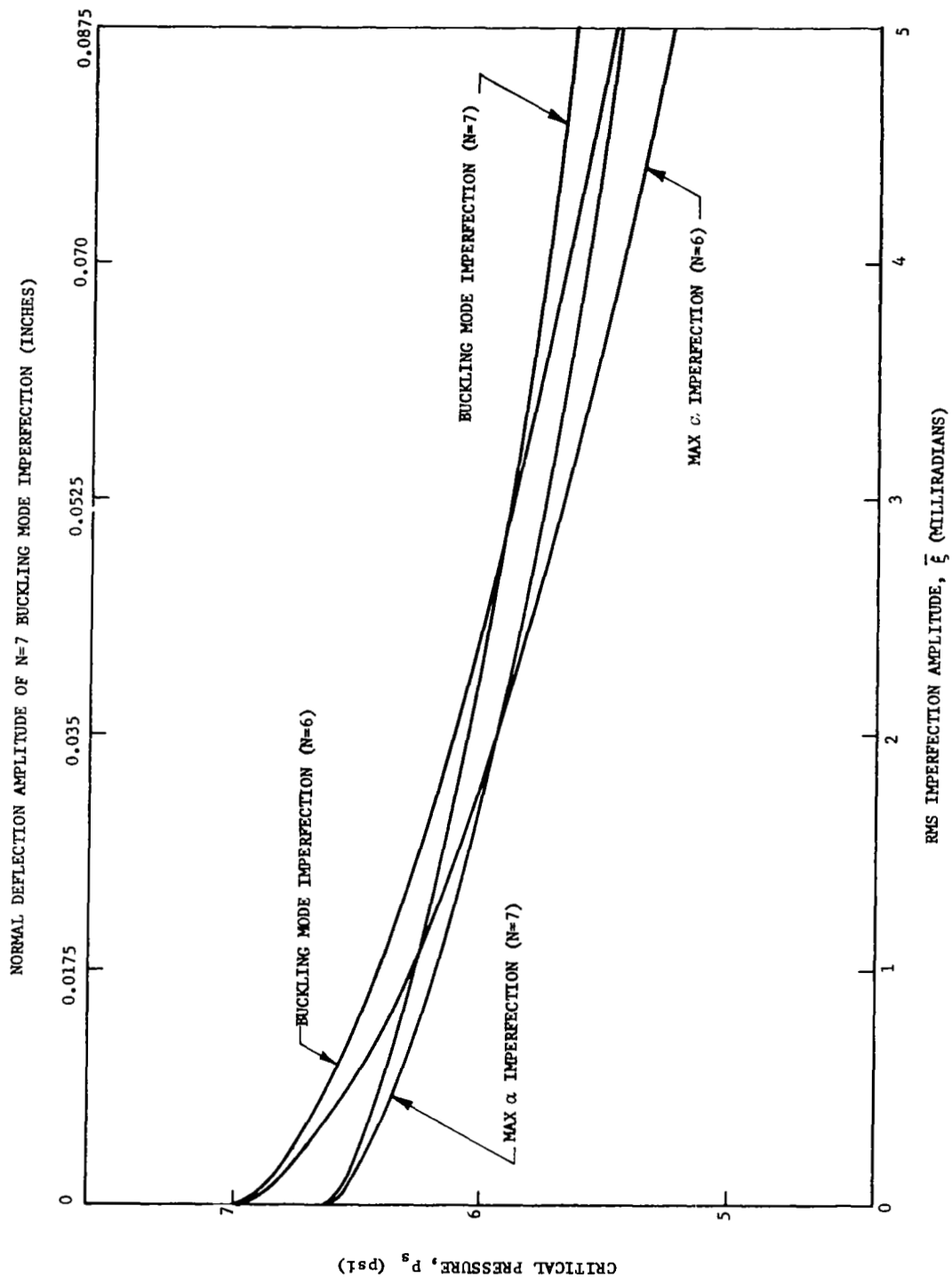

FIGURE 2. 120-DEGREE SANDWICH CONE (REFERENCE 15)

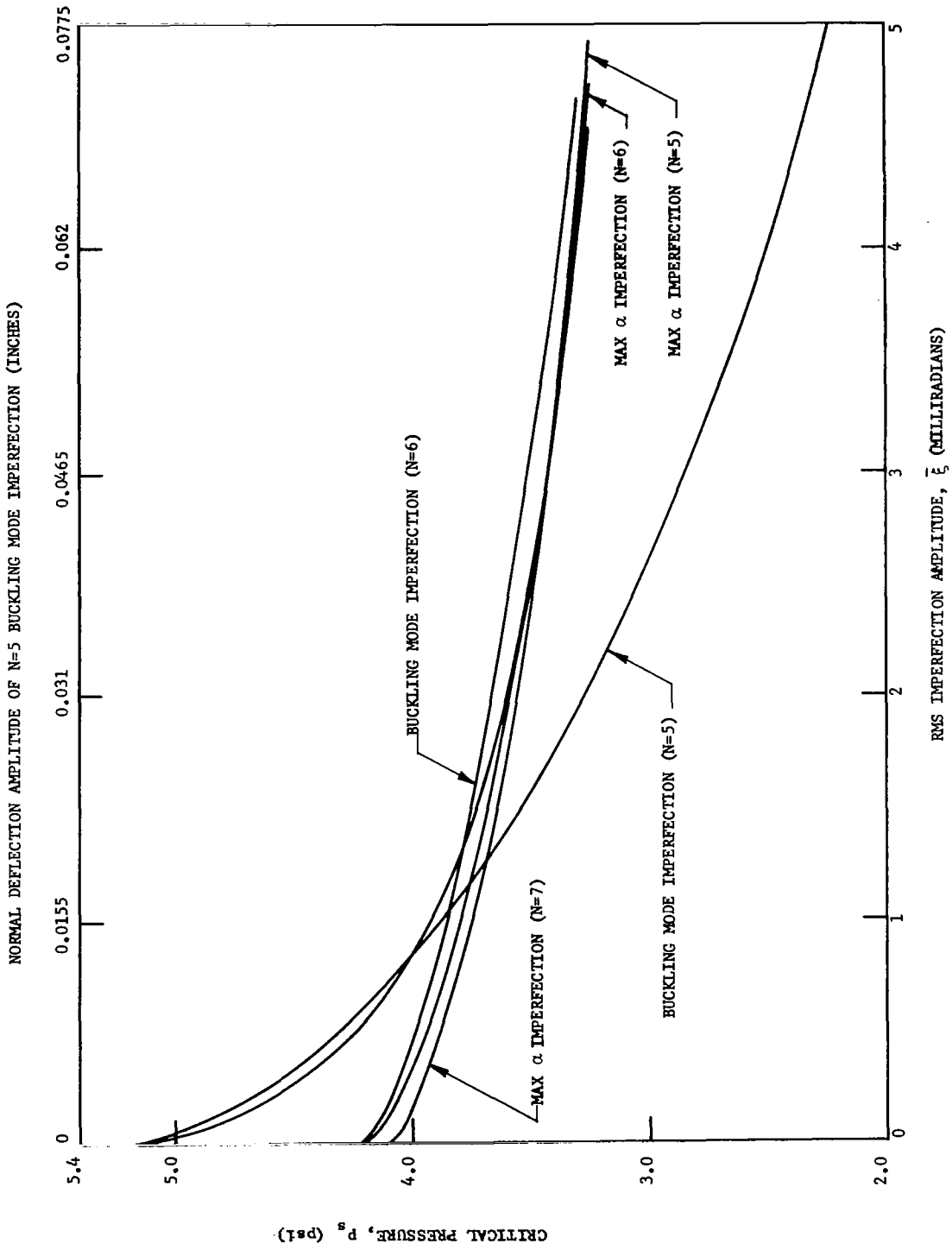

FIGURE 3. 120-DEGREE RING-STIFFENED CONE (REFERENCE 15)

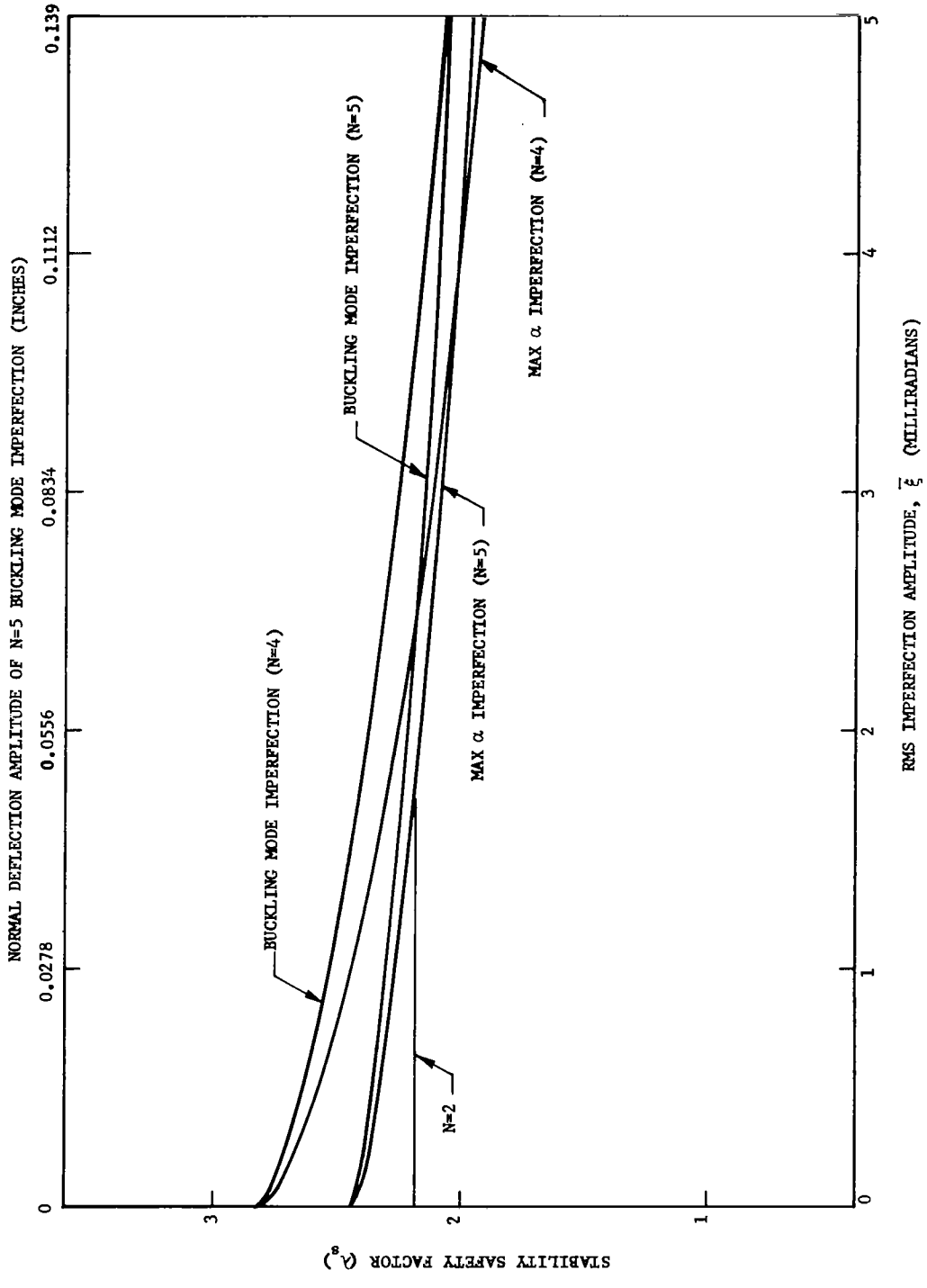

FIGURE 4. 120-DEGREE SANDWICH CONE (REFERENCE 16)

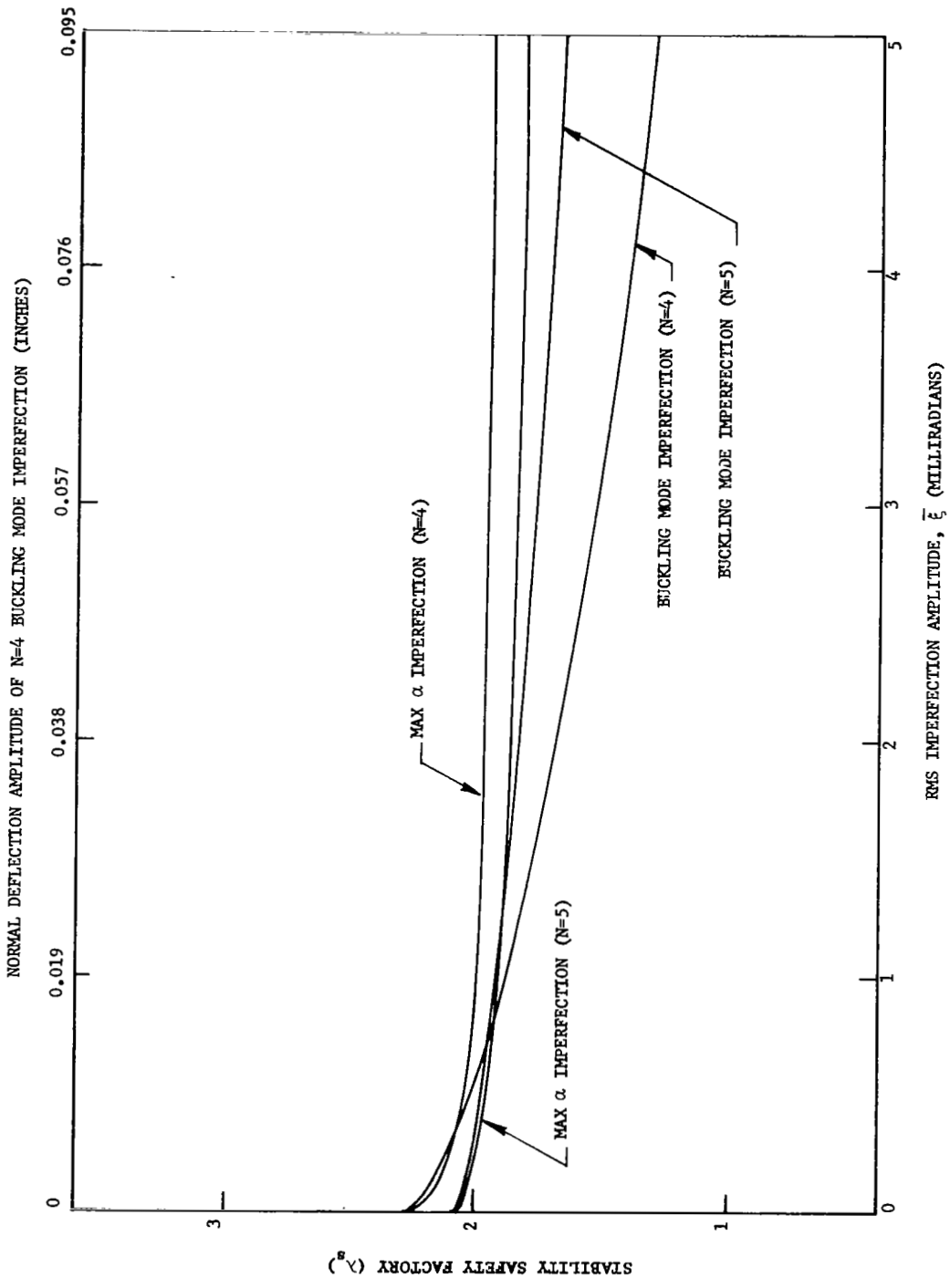

FIGURE 5. 120-DEGREE RING-STIFFENED CONE (REFERENCE 16)

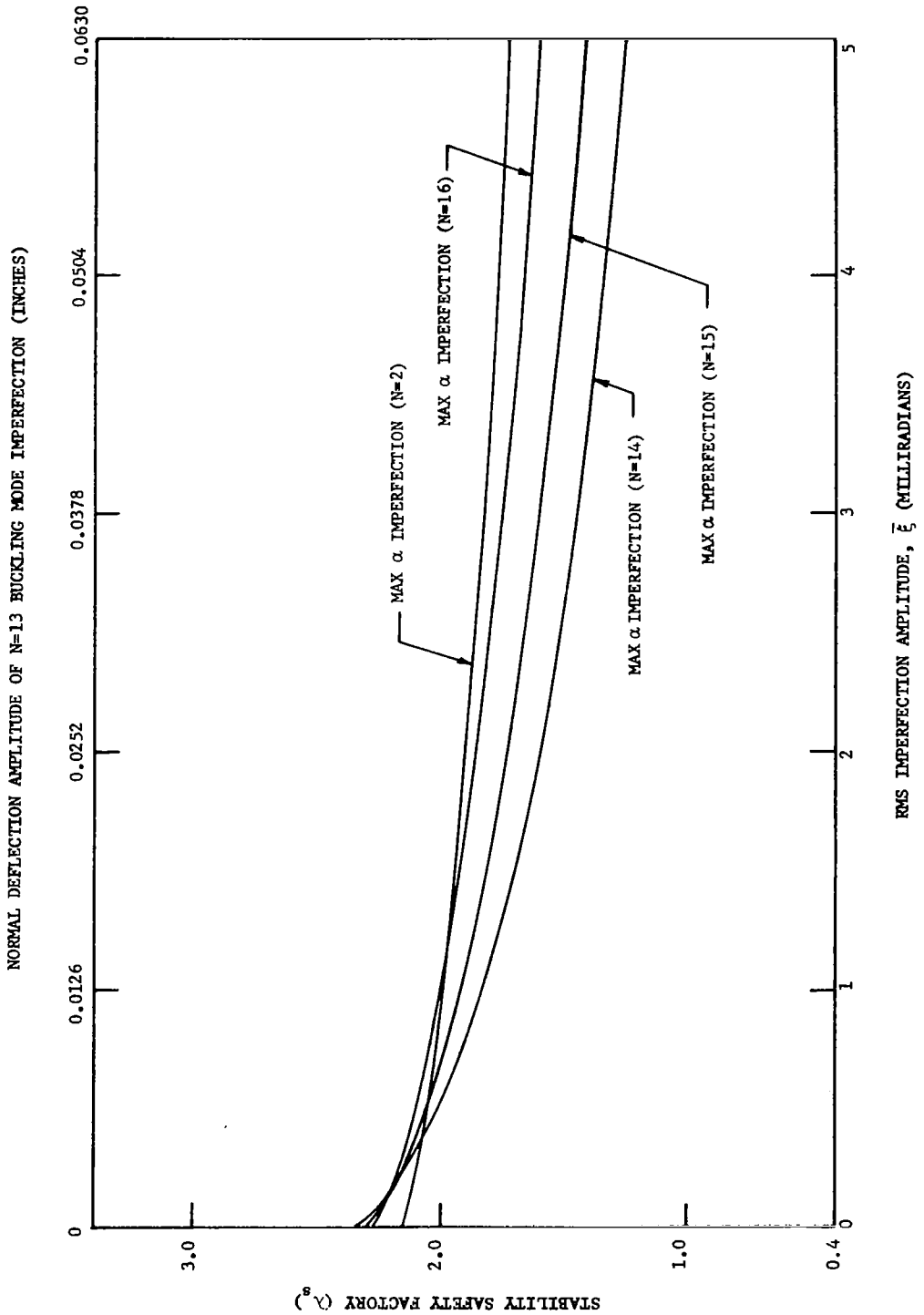

FIGURE 6. OA.833 TENSION SHELL (REFERENCE 16)

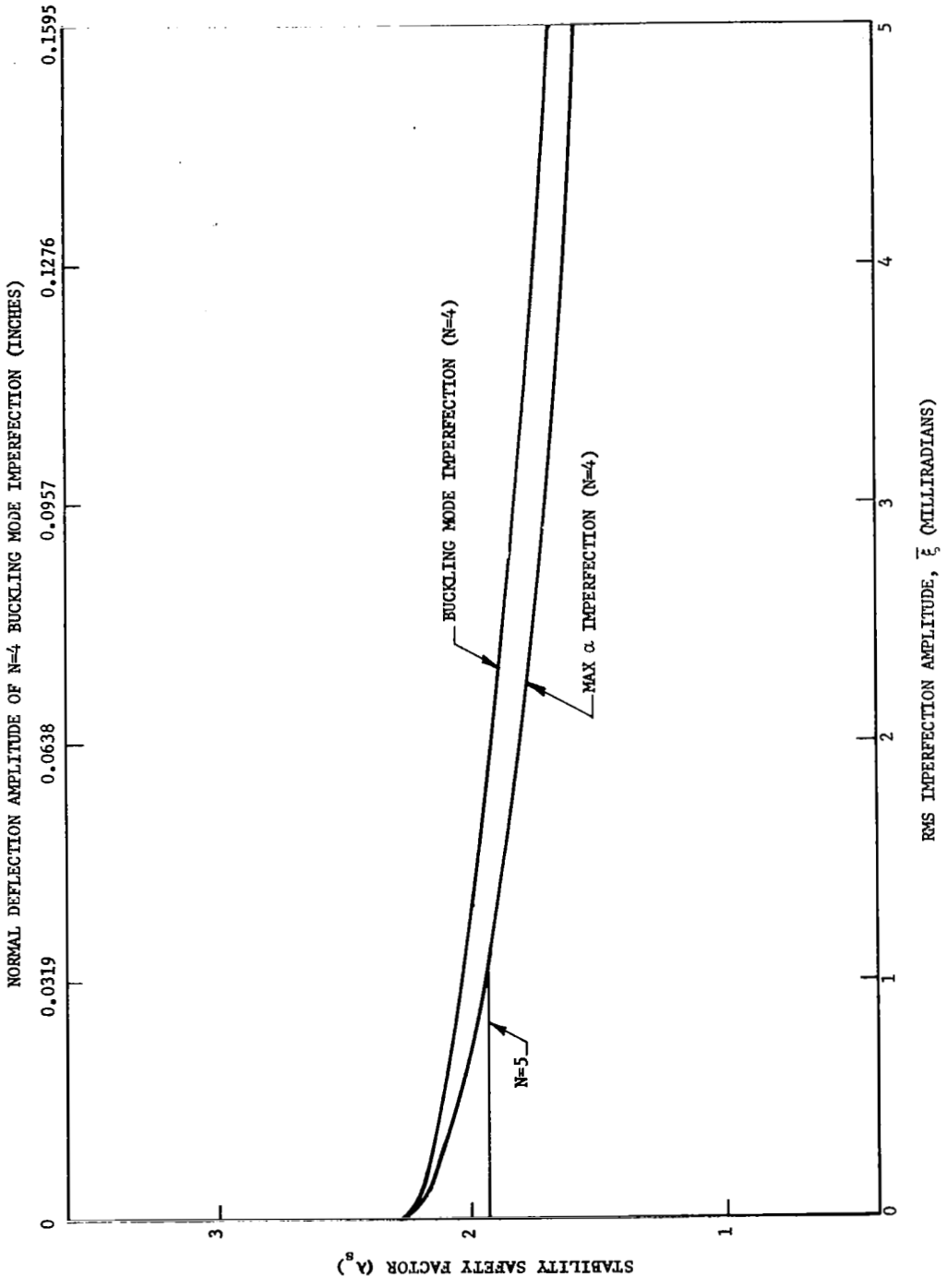

FIGURE 7. 140-DEGREE SANDWICH CONE (REFERENCE 17)

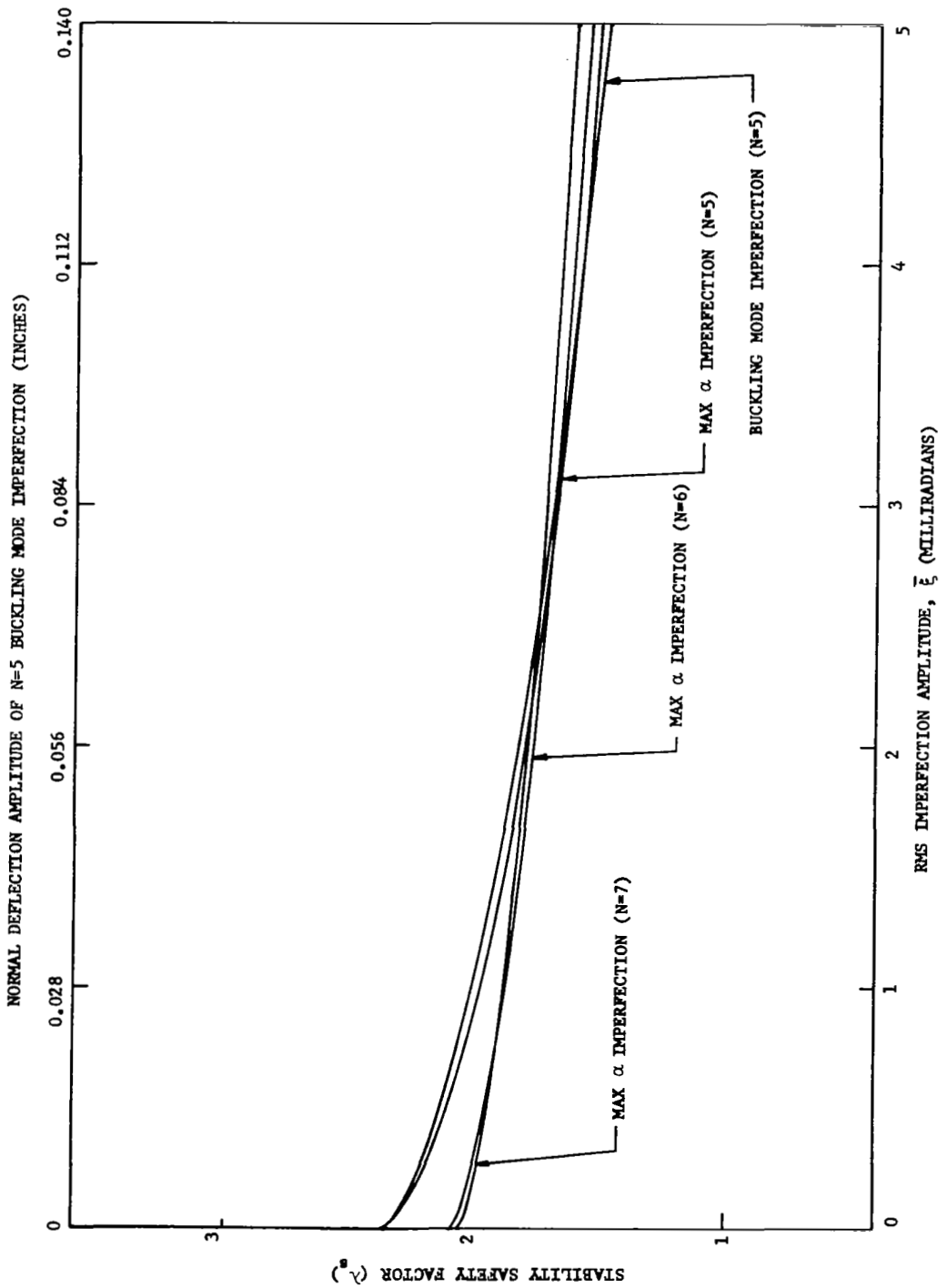

FIGURE 8. 60 DEGREE SPHERICAL DISH (REFERENCE 17)

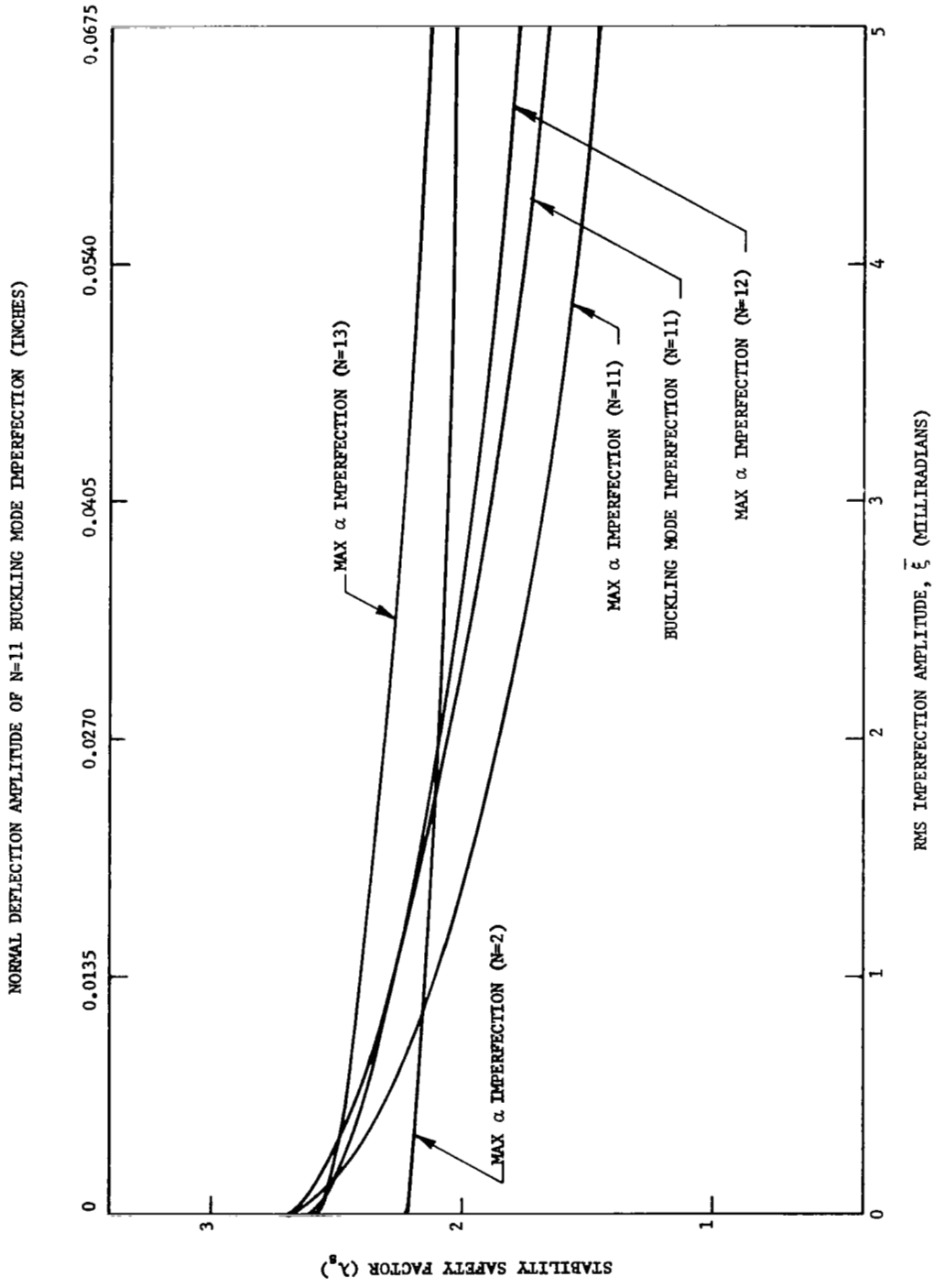

FIGURE 9. OA .65 TENSION SHELL (REFERENCE 17)